OPEN ACCESS
Journal of Multidisciplinary Applied Natural Science Vol. xx No. xx (xxxx) https://doi.org/10.47352/jmans.2774-3047.460
Check for updates
Research Article

Eugenol-Derived *N*-(3-aminopropyl)-2-(4-allyl-2-methoxyphenoxy)acetamide as a Selective Receptor for Cyanide and Dihydrogen Phosphate: Spectroscopic and Computational Insights

Venty Suryanti*, Laras Ayu Wijayanti, Yoga Royandana Firdaus, Fajar Rakhman Wibowo, and Ahmad Marzuki

Received : March 1, 2026	Revised : May 17, 2026	Accepted : May 21, 2026	Online : July 23, 2026

Abstract
The compound *N*-(3-aminopropyl)-2-(4-allyl-2-methoxyphenoxy)acetamide (**4**) was synthesized from eugenol through a three-step reaction. Possessing both amide and amine groups, the molecule provides effective hydrogen-bond donor sites suitable for anion recognition. The binding behaviour of compound **4** toward F^-, CN^-, AcO^-, SO_4^{2-}, and $H_2PO_4^-$ was examined using ^{1}H-NMR spectroscopy. No significant spectral changes were observed upon addition of F^-, AcO^-, or SO_4^{2-}, indicating minimal or no interaction. In contrast, the introduction of CN^- and $H_2PO_4^-$ produced notable chemical shift variations, consistent with hydrogen-bond formation and host-guest complexation. To further elucidate these interactions, density functional theory (DFT) calculations were performed at the aug-cc-pVDZ level. Computational models revealed that F^- and AcO^- induce cleavage of the amide N–H bond through strong hydrogen bonding and partial covalent character, whereas CN^- and $H_2PO_4^-$ primarily engage in hydrogen-bonding interactions without bond cleavage. Gauge-independent atomic orbital (GIAO) calculations predicted substantial downfield shifts of the amide proton, from 4.72 ppm in the free receptor to 15.5, 10.89, 16.54, and 12.27 ppm for F^-, CN^-, AcO^-, and $H_2PO_4^-$, respectively. Overall, both experimental and computational findings demonstrate that compound **4** functions as an effective receptor for CN^- and $H_2PO_4^-$, with strong theoretical binding responses also observed for F^- and AcO^-.

Keywords: amide compound, anion recognition, Density Functional Theory (DFT), eugenol-derived receptor, host-guest complexation

1. INTRODUCTION

The recognition and sensing of anions have received considerable attention in supramolecular chemistry due to their essential roles in biological systems, environmental processes, and industrial applications [1]-[3]. Anions such as cyanide (CN^-) and dihydrogen phosphate ($H_2PO_4^-$) are of particular interest because of their contrasting chemical properties and environmental relevance. The CN^- is a highly toxic anion frequently encountered in industrial effluents, while phosphate plays a vital role in biological and agricultural systems. The selective detection and binding of these anions are therefore important for both environmental monitoring and biological regulation [4]-[8].

Molecular receptors designed for anion recognition typically rely on non-covalent interactions such as hydrogen bonding, electrostatic attraction, and π-anion interactions [9]-[13]. Among these, hydrogen bonding remains one of the most versatile and widely employed strategies for anion binding. Receptors containing amide and amine groups are especially effective because they offer multiple hydrogen-bond donor sites capable of interacting with various anionic species. Structural modification of such receptors allows fine-tuning of their binding affinity and selectivity toward specific anions [14]-[18]. For example, amide-based receptors often exhibit strong binding toward oxoanions, such as $H_2PO_4^-$ and SO_4^{2-}, through bidentate hydrogen bonding, whereas amine-containing systems can provide complementary binding sites and improve solubility in organic media [19]-[21]. The combination of both amide and amine functionalities within a single molecule has been shown to create cooperative binding sites, thereby strengthening host-guest interactions and improving anion discrimination [2]. Such dual-function receptors are also advantageous because

Please cite this article as: V. Suryanti, L. A. Wijayanti, Y. R. Firdaus, F. R. Wibowo, and A. Marzuki. (2026). "Eugenol-Derived N-(3-aminopropyl)-2-(4-allyl-2-methoxyphenoxy)acetamide as a Selective Receptor for Cyanide and Dihydrogen Phosphate: Spectroscopic and Computational Insights ". *Journal of Multidisciplinary Applied Natural Science*. https://doi.org/10.47352/jmans.2774-3047.460

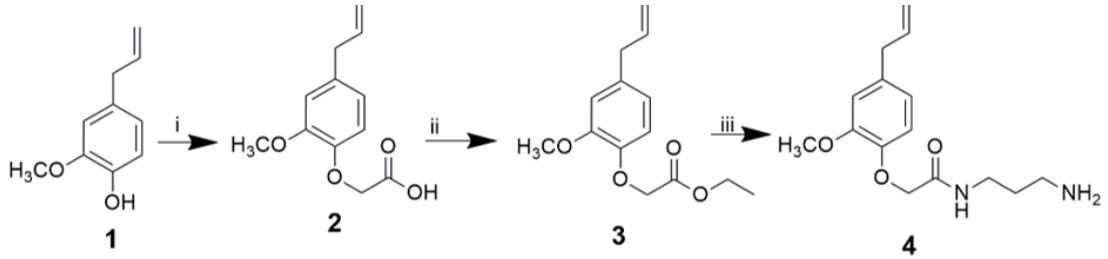

Figure 1. Reaction steps for synthesising of *N*-(3-aminopropyl)-2-(4-allyl-2-methoxyphenoxy)acetamide (**4**) from eugenol (**1**). Reagents and conditions: (i). (a). NaOH, 30 min, r.t; (b). $ClCH_2COOH$, 2 h at 80 °C; (c). 6 M HCl, (ii).CH_3CH_2OH, HCl, reflux, 6 h, (iii). $H_2N(CH_2)_3NH_2$, CH_2Cl_2, reflux, 48 h [28].

they can participate in proton-transfer equilibria, allowing both hydrogen bonding and deprotonation pathways to contribute to anion sensing [14].

Natural compounds have used as starting materials for synthesising of anion receptor [22]-[27]. The *N*-(3-aminopropyl)-2-(4-allyl-2-methoxyphenoxy)acetamide (**4**) was synthesised from eugenol through a three-step reaction pathway (Figure 1) [28]. In this study, we investigate the anion recognition properties of compound **4**, a receptor designed to incorporate both amide and amine hydrogen-bond donor sites. The binding behavior of compound **4** toward a series of representative anions, such as F^-, CN^-, AcO^-, SO_4^{2-}, and $H_2PO_4^-$, was examined using ^{1}H-NMR spectroscopy. Owing to its sensitivity to local electronic environments, ^{1}H-NMR serves as a powerful analytical tool for probing hydrogen bonding, proton transfer, and structural rearrangements during receptor-anion interactions [29]. Changes in chemical shifts or the emergence and disappearance of proton signals provide direct evidence of complex formation, deprotonation events, and conformational adjustments within the receptor framework. This work aims to elucidate the binding modes, selectivity, and potential proton abstraction processes associated with anion coordination to compound **4**, thereby advancing the understanding of simple amide-amine systems in anion recognition chemistry. To complement the experimental findings, density functional theory (DFT) calculations were employed to model the structural and electronic features of the receptor-anion complexes. The combined experimental and theoretical insights offer a deeper understanding of the interaction mechanisms and provide a foundation for the rational design of improved receptor molecules for selective sensing and separation applications [30]-[34].

2. MATERIALS AND METHODS

2.1. Materials

Eugenol was purchased from PT Indesso Aroma, Purwokerto, Indonesia. Sodium hydroxide (NaOH), hydrochloric acid (HCl), chloroacetic acid, sodium hydrogen carbonate ($NaHCO_3$), anhydrous magnesium sulfate ($MgSO_4$), 1,3-diaminopropane, diethyl ether, dichloromethane, *n*-hexane, ethanol, deuterated chloroform ($CDCl_3$), and tetrabutylammonium (TBA) salts (such as CN^-, F^-, $H_2PO_4^-$, AcO^- and SO_4^{2-}) were purchased from Sigma-Aldrich.

2.2. Methods

2.2.1. Synthesis of N-(3-aminopropyl)-2-(4-allyl-2-methoxyphenoxy)acetamide (4)

Compound **4** was synthesized from eugenol following a reported procedure [28]. Eugenol (5.0 g) was stirred with NaOH solution (17.5 mL, 33% w/v) for 30 min, followed by the slow addition of chloroacetic acid (12.5 mL, 50% w/v). The mixture was heated at 80 °C for 2 h, cooled, and acidified to pH 1 with 6 M HCl. The precipitate was filtered, extracted with diethyl ether, re-acidified, and dried to give compound **2**. Then, compound **2** (7 mmol) was refluxed with ethanol (15.5 g) and saturated HCl (0.5 g) for 6 h. After evaporation, the residue was extracted with water and diethyl ether, washed with saturated $NaHCO_3$, dried over anhydrous $MgSO_4$, and concentrated to yield compound **3**. Then, compound **3** (1 mmol) and 1,3-diaminopropane (1.2 mmol) in dichloromethane (50

mL) were refluxed for 48 h. The solvent was removed, and the residue was purified by column chromatography (*n*-hexane/ethanol = 97:3) to afford compound **4** as a brown powder.

*2.2.2. Anion Recognition Studies of Compound **4** by ^{1}H-NMR Spectroscopy*

Compound **4** (5 mg) was dissolved in $CDCl_3$ to prepare a 0.1 M of solution **4**. This solution was subsequently diluted with $CDCl_3$ to obtain a final concentration of 0.0167 M in 600 µL (corresponding to 10^{-5} mol). The anions (CN^-, F^-, $H_2PO_4^-$, AcO^- and SO_4^{2-}), in the form of their TBA salts, were dissolved in $CDCl_3$ to prepare 1 M anion stock solutions. A solution of compound **4** in $CDCl_3$ (1×10^{-5} mol) was placed in an NMR tube. Subsequently, aliquots of the anion salt solutions were added to achieve varying molar ratios of 0, 0.5, 1, 1.5, 2, 5, 8, and 15 equivalents relative to compound **4**. The resulting mixtures were analyzed by ^{1}H NMR spectroscopy to evaluate the interaction between compound ***1*** and the anions.

*2.2.3. Computational Studies of Compound **4***

The receptor compound **4** was optimized by first constructing its molecular structure using GaussView 5. Initial geometry optimization and conformational analysis were performed using the Hartree–Fock (HF) method with the 6-311G** basis set. The HF method was selected for the preliminary conformational search because it provides computational efficiency and reliable structural optimization for generating low-energy conformers. Geometry optimization was performed at the HF/6-311G** level of theory. A conformational scan was then carried out by rotating the dihedral angle of the aliphatic chain in 5° increments over a full 360° rotation. The resulting structures were saved as *.gjf* files and computed using Gaussian with the same HF/6-311G** method. The generated log files were subsequently analyzed, yielding several local minimum-energy conformations of compound **4** to be used in the next stages of the study.

Several local minimum structures obtained from the conformational scan of compound **4** then were subjected to hydrogen abstraction by removing the amide hydrogen atom. These modified structures were calculated using GaussView 5 at the HF/6-311G** level of theory. The resulting log files were used for subsequent NMR and UV–Vis characterizations. The abstraction process produced four distinct stability states of compound **4**, determined based on their relative energy differences and corresponding Boltzmann populations. The structure selected was the one with the lowest energy identified during the initial scan, with priority given to the conformation exhibiting the highest Boltzmann population after hydrogen abstraction.

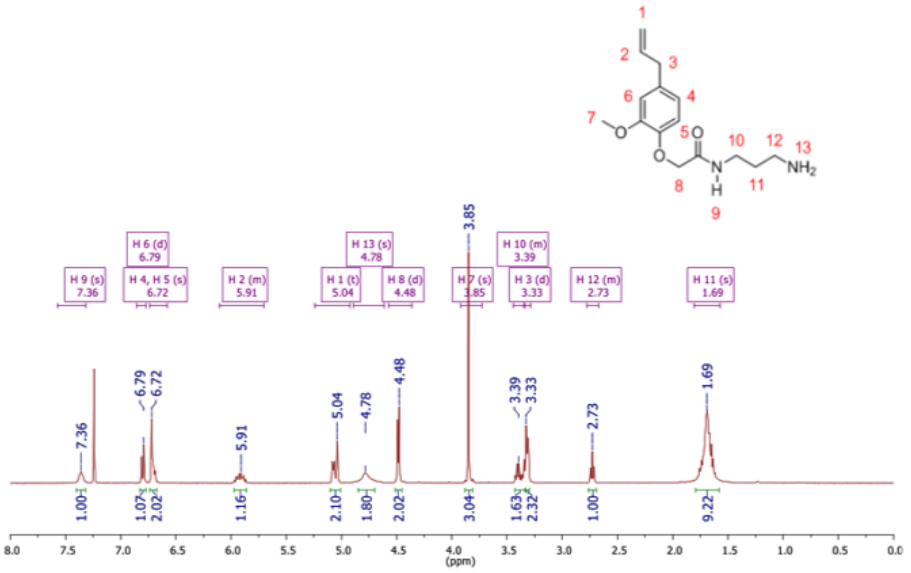

Figure 2. ^{1}H-NMR spectrum of compound **4**.

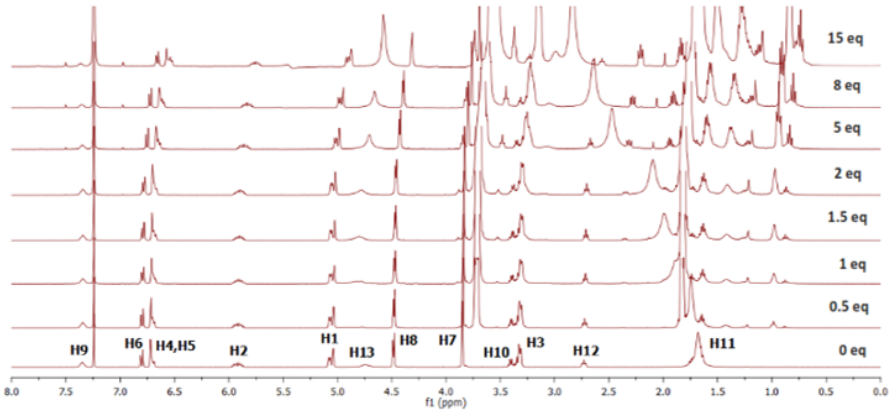

Figure 3. ^{1}H-NMR spectra of compound **4** upon addition of F^- anion.

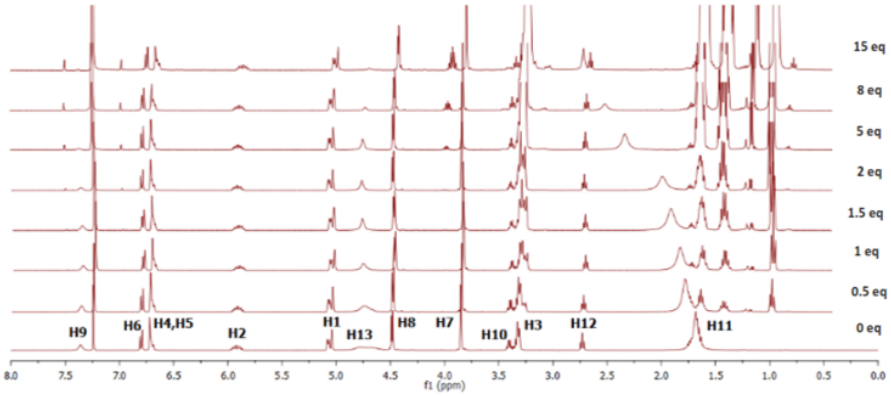

Figure 4. ^{1}H-NMR spectra of compound **4** upon addition of CN^- anion.

The most stable conformation of compound **4** was then modelled in complexes with the anions. These interactions were calculated using the ONIOM method, which allows different regions of a molecular system to be treated at different levels of theory to balance computational accuracy and cost. The interacting region between the receptor and anion was treated using DFT/cc-pVDZ level because DFT provides improved accuracy for describing hydrogen-bonding and electronic interactions. The remaining non-interacting portion of the receptor was treated at the HF/6-311G(d,p) level. Geometry optimization, interaction energy analysis, Gauge-independent atomic orbital (GIAO) NMR calculations, and time-dependent DFT (TD-DFT) UV–Vis predictions were subsequently performed on the optimized complexes.

3. RESULTS AND DISCUSSIONS

3.1. Synthesis of Compound 4

Compound **4** was synthesized from eugenol through a three-step reaction sequence. Compound **2** was obtained as white crystals with a yield of 72% and a melting point of 91 °C, while compound **3** was synthesised as a brown liquid with a yield of 76%. The reaction of compound **3** with 1,3-diaminopropane via amidation afforded compound **4** as a brownish-yellow solid in 88% yield with a melting point of 82 °C. The ^{1}H NMR spectra of the synthesized compounds were consistent with those reported in the literature (Figure 2) [28].

The ^{1}H NMR spectrum of compound **4** ($CDCl_3$, 400 MHz) showed the following chemical shifts (in ppm): δ 5.13–4.97 (*d*, 2H, C=CH_2), 6.00–5.81 (*m*, 1H, C=CH-C), 3.33 (*d*, *J* = 6.7 Hz, 2H, C-CH_2-Ar), 6.73–6.62 (*s*, 2H, Ar-H), 6.79 (*d*, *J* = 8.0 Hz, 1H, Ar-H), 3.85 (*s*, 3H, O-CH_3), 4.48 (*d*, *J* = 11.8 Hz, 2H, O-CH_2-C), 7.36 (*s*, 1H, NH), 3.39 (*m*, *J* = 11.5, 5.8 Hz, 2H, N-CH_2-C), 1.69 (overlapping water peak), 2.73 (*m*, 2H, C-CH_2-N), and 4.78 (*s,* 2H, NH_2). The appearance of the NH proton at δ 7.36 ppm and the NH_2 proton at δ 4.78 ppm, together

with the absence of ethyl group signals (O–CH_2CH_3) at δ 4.24 and 1.26 ppm, confirms the successful conversion of compound **3** into compound **4**.

3. 2. Anion Recognition Studies by ^{1}H-NMR Spectroscopy

Compound **4** and anion salts (TBA) were dissolved in $CDCl_3$. This polar aprotic solvent lacks hydroxyl groups. Hydroxyl groups of solvent can interfere with hydrogen bonding between the receptor and the anion. Moreover, solvents that do not solvate anions enhance the nucleophilicity of the anion. Therefore, the use of $CDCl_3$ as a solvent prevents disruption of the hydrogen bonds formed between compound **4** and the anion while maintaining the anion's nucleophilicity. Anions were added to solution **4** in varying mole equivalents ranging from 0 to 15. The anions, which are F^-, CN^-, AcO^-, SO_4^{2-}, and $H_2PO_4^-$, were introduced in the form of quaternary ammonium salts. The anions in this form are more easily ionized and dissociate readily from the salt matrix. The resulting mixtures of solution **4** with each anion were subsequently analyzed using ^{1}H-NMR spectroscopy.

3.2.1. Anion Recognition Studied for F^- and CN^- by ^{1}H-NMR Spectroscopy.

Different mole equivalents of anions (0–15

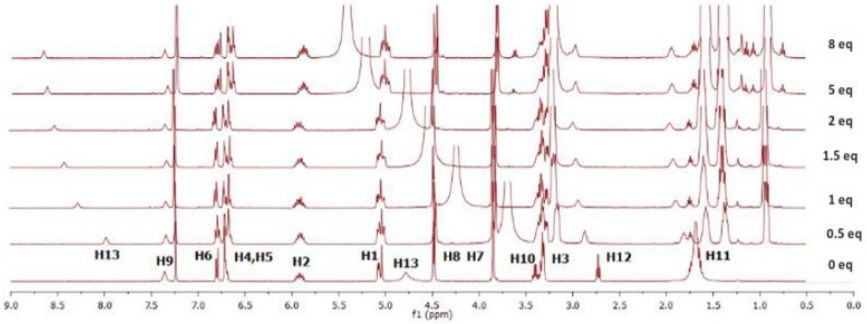

Figure 5. ^{1}H-NMR spectra of compound **4** upon addition of $H_2PO_4^-$ anion.

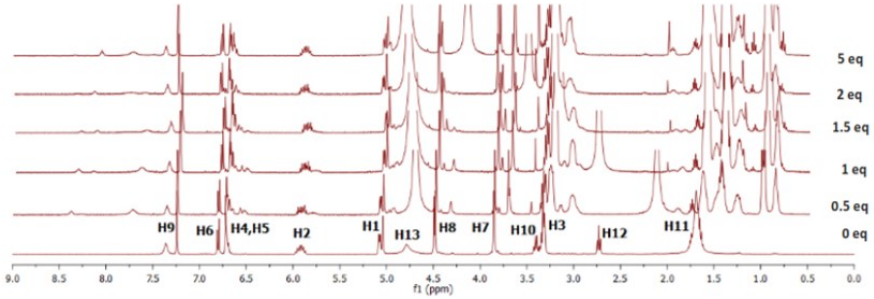

Figure 6. ^{1}H-NMR spectra of compound **4** upon addition of SO_4^{2-} anion.

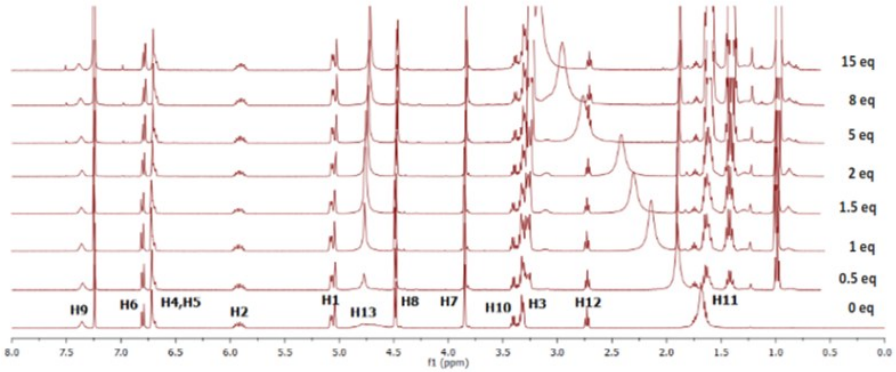

Figure 7. ^{1}H-NMR spectra of compound **4** upon addition of AcO^- anion.

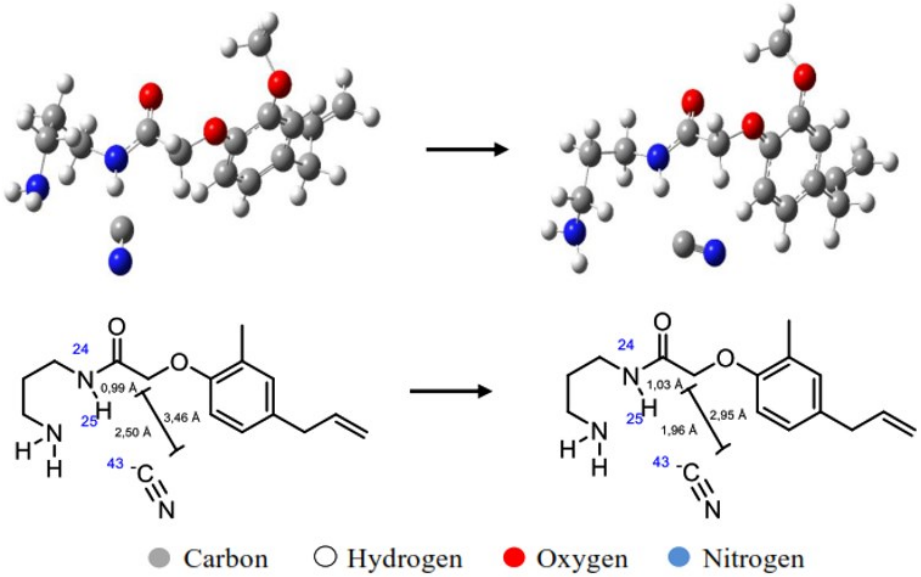

Figure 8. Compound **4** interacting with the CN^- anion in three-dimensional representation (upper) and two-dimensional representation (lower).

Table 1. Bond distances between compound **4** and the CN^- anion.

Bonding	Initial Distance (Å)	Optimize Distance (Å)
24 (N) to 25 (H)	0.99	1.03
43 (C) to 25 (H)	2.50	1.96
24 (N) to 43 (C)	3.46	2.95

equivalents) were added to solution **4** and the corresponding changes in the ^1H NMR spectra were monitored to evaluate the binding interaction between compound **4** and the anions. Chemical shift variations were observed, indicating the formation of hydrogen-bonding interactions between the receptor **4** and the anions. The detailed ^1H NMR spectral changes are presented in Figures 3 and 4. These figures show downfield shifts in the proton peaks. The peak at 1.69 ppm shifts significantly, corresponding to the water impurity signal, which overlaps with the H11 proton peak. The presence of this water signal in the ^1H NMR spectrum of compound **4** is likely due to residual moisture in the $CDCl_3$ solvent used to dissolve compound **4** and the TBA salts. The $CDCl_3$ solvent employed has a stated purity of 99.8%, which contains approximately 0.01% water. This trace amount of water can interfere with the interaction between the anion and compound **4**. Because water is a protic solvent, it can solvate anions and thereby decrease their effective nucleophilicity. The observed downfield shift of the water peak indicates an interaction between the water molecules and the added anions. Such interactions render the water protons less shielded, resulting in a downfield shift of their signal.

Despite the presence of water in the system, compound **4** remain capable of interacting with the added CN^- anion through the amide NH (H9) and amine NH_2 (H13) groups. Compound **4** does not interact with F^-, as evidenced by the absence of any shift in the H9 and H13 proton signals. In contrast, upon the addition of CN^-, the NH and NH_2 groups undergo deprotonation, indicated by the disappearance of the H9 and H13 peaks in the ^1H NMR spectra. Upon the addition of 5 equivalents of CN^-, the intensity of the H9 proton peak began to decrease, and the peak completely disappeared after the addition of 8 equivalents of CN^-. The disappearance of the H9 signal indicates deprotonation or bond cleavage at the NH group. Subsequently, deprotonation of the NH_2 group commenced following the deprotonation of the NH

group. As shown in Figure 4, when 8 equivalents of CN^- were added, the H13 proton peak began to diminish in intensity and completely disappeared after the addition of 15 equivalents of CN^-.

The CN^- anion can form hydrogen bonds with the NH and NH_2 groups of compound **4** and is capable of deprotonating the hydrogen atoms of these groups. This occurs because CN^- possesses a higher basicity than F^-. Consequently, CN^- more effectively attracts hydrogen atoms from both donor sites. In general, the greater the basicity of an anion, the stronger its ability to act as a hydrogen-bond acceptor. Hydrogen bonding arises from proton transfer between donor and acceptor atoms, and higher basicity facilitates this transfer, thereby strengthening the interaction [35]. Stronger hydrogen-bond interactions, in turn, enhance π-electron delocalization and promote deprotonation [11][36]. Consistent with these findings, previous research by Odago *et al.* [37] also demonstrated receptor selectivity toward CN^- over F^-, attributable to the higher basicity of the cyanide anion.

Compound **4** initially interacts with CN^- through hydrogen-bonding interactions with the NH (H9) and NH_2 (H13) groups, indicating a supramolecular recognition process at lower anion equivalents. At higher CN^- concentrations, this interaction proceeds to deprotonation of these groups, as evidenced by the disappearance of the corresponding ^{1}H-NMR signals. Thus, the overall process involves initial hydrogen bonding followed by acid-base deprotonation. Although HCN formation is possible, it was not directly confirmed in this study. No corresponding HCN signal was observed in the ^{1}H-NMR spectra; typically, the HCN proton signal appears at δ ~6–7 ppm. Therefore, no definitive assignment of HCN formation is made.

3.2.2. Anion Recognition Studied for Oxyanion ($H_2PO_4^-$, SO_4^{2-}, and AcO^-) by ^{1}H-NMR Spectroscopy

The mole equivalents of AcO^- added to solution **4** were 0.5-15 equivalents. However, the addition of SO_4^{2-} was limited to 5 equivalents, as most of the proton peaks of compound **4** were obscured by the TBA signals, making the chemical shifts less discernible. In contrast, $H_2PO_4^-$ was added only up to 8 equivalents because further additions produced no significant spectral changes. The ^{1}H-NMR spectra shows noticeable shifts following the addition of oxyanions (Figures 5, 6 and 7). Similar to the results for F^- and CN^-, the addition of AcO^-, SO_4^{2-}, and $H_2PO_4^-$ also produced a water impurity peak at approximately 1.69 ppm in the spectrum of compound **4**. This water signal likely originated from residual moisture in the $CDCl_3$ solvent and from the TBA salts used, as the TBA acetate and TBA sulfate solutions were prepared in water at concentrations of 1.0 M and 0.86 M, respectively.

Despite the presence of water, the amide NH (H9) and amine NH_2 (H13) groups of compound **4** remain capable of interacting with the added $H_2PO_4^-$ anion. It was observed that the addition of $H_2PO_4^-$, SO_4^{2-}, and AcO^- did not cause any shift in the NH (H9) proton signal, which indicates that no interaction occurs between the NH group and the oxyanions. The shift of the H13 proton after the addition of SO_4^{2-} could not be evaluated because the H13 peak was obscured by the TBA signal. Following the addition of AcO^-, the H13 peak also remained unchanged, suggesting no interaction between the NH_2 group and AcO^-. In contrast, upon addition of $H_2PO_4^-$, the H13 signal exhibited a pronounced downfield shift. A noticeable shift in the H13 proton peak was already evident after the addition of 0.5 mol equivalents of $H_2PO_4^-$, indicating that compound **4** can interact with $H_2PO_4^-$ and effectively compete with water molecules. However, compound **4** was unable to bind all the added $H_2PO_4^-$, as evidenced by the concurrent shift in the water proton peak upon addition of 0.5 mol equivalents of the anion. The H13 peak shifted significantly downfield by 3.88 ppm, from 4.78 ppm to 8.66 ppm (Figure 5). The pronounced downfield shift of the H13 peak indicates the formation of a strong hydrogen bond between the hydrogen atoms of the NH_2 group and the $H_2PO_4^-$ anion.

In addition, the H11 and H12 proton signals (corresponding to CH_2 groups) also shifted downfield, with the H11 peak moving by 0.26 ppm (from 1.69 to 1.95 ppm) and the H12 peak shifting by 0.25 ppm (from 2.73 to 2.98 ppm). These shifts suggest that the CH_2 groups also participate in hydrogen bonding interactions with $H_2PO_4^-$. After the addition of 2 equivalents of $H_2PO_4^-$, the H11, H12, and H13 peaks no longer exhibited significant shifts, indicating that compound **4** had reached

saturation in its interaction with the anion. These three proton signals remained observable even after the addition of 8 equivalents, suggesting that no deprotonation occurred in compound **4**.

Compound **4** does not exhibit any interaction with AcO^-, even though AcO^- possesses a higher basicity than $H_2PO_4^-$. This phenomenon may be attributed to the greater bond energy required for compound **4** to interact with $H_2PO_4^-$ compared to AcO^-. The higher bond energy corresponds to stronger binding affinity, allowing $H_2PO_4^-$ to form more stable interactions despite being less basic and larger in size [38]. Moreover, the difference in molecular geometry between the two anions also influences their binding behavior: AcO^- adopts a trigonal planar geometry, whereas $H_2PO_4^-$ has a tetrahedral structure [39]. The tetrahedral geometry of $H_2PO_4^-$, containing four oxygen atoms, enables the formation of multiple hydrogen bonds, thereby enhancing its interaction potential compared to other anions [40].

Based on the analysis results, compound **4** is capable of interacting with CN^- and $H_2PO_4^-$ through different mechanisms. Upon the addition of CN^-, compound **4** undergoes deprotonation at both the amide NH (H9) and amine NH_2 (H13) groups. In contrast, the addition of $H_2PO_4^-$ does not cause deprotonation of these groups; instead, hydrogen bonding occurs between the NH_2 and alkyl CH_2 (H11 and H12) protons of compound **4** and the oxygen atoms of $H_2PO_4^-$. These differences in interaction arise from the distinct basicity and electronegativity characteristics of the two anions. The CN^- anion, with its higher basicity, tends to abstract hydrogen atoms, leading to deprotonation, whereas the more electronegative $H_2PO_4^-$ favors the formation of hydrogen bonds [41].

The interaction between compound **4** and the investigated anions is governed by both intrinsic anion basicity and solvation effects. In solution, solvent molecules and trace water compete for hydrogen bonding, reducing the effective availability and basicity of the anions for binding. This competitive solvation weakens anion–receptor interactions by stabilizing solvated anion clusters. Accordingly, fluoride shows minimal interaction

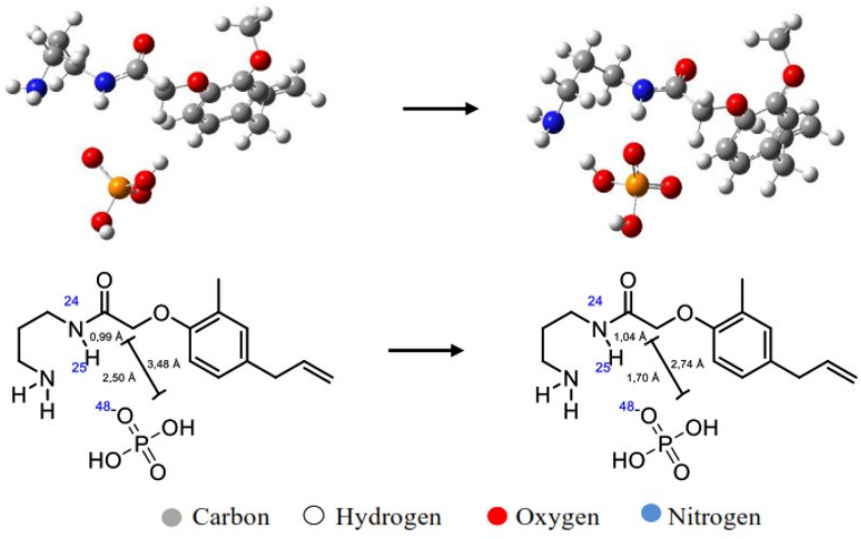

Figure 9. Compound **4** interacting with the $H_2PO_4^-$ anion in three-dimensional representation (upper) and two-dimensional representation (lower).

Table 2. Bond distances between compound **4** and the $H_2PO_4^-$ anion.

Bonding	Initial Distance (Å)	Optimize Distance (Å)
24 (N) to 25 (H)	0.99	1.04
45 (O) to 25 (H)	2.50	1.70
24 (N) to 45 (O)	3.48	2.74

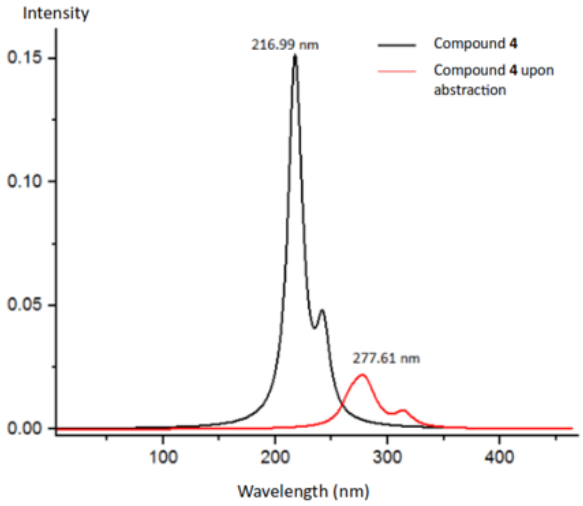

Figure 10. Theoretical UV-vis spectra of compound **4** upon hydrogen abstraction.

due to strong hydration, while cyanide can partially overcome solvation, resulting in initial hydrogen bonding followed by deprotonation at higher concentrations. For oxyanions ($H_2PO_4^-$, SO_4^{2-}, and AcO^-), strong solvation and charge delocalization further reduce their effective basicity, leading to weaker interactions, particularly for SO_4^{2-}. Overall, the binding behavior reflects a balance between anion basicity and solvation effects rather than basicity alone.

Quantitative ^{1}H-NMR titration analysis was not conducted, as reliable determination of binding constants was not possible under the present conditions due to significant spectral limitations. These include signal overlap with TBA counterions, interference from trace water, and peak broadening or disappearance upon deprotonation in the case of strongly interacting anions such as CN^-, all of which prevent accurate integration and fitting. Therefore, the analysis is based on qualitative ^{1}H-NMR observations. Nevertheless, the systematic chemical shift changes and signal variations provide consistent evidence for anion-dependent interaction behavior. To further confirm the binding model of compound **4** with anions, computational studies was carried out, as ^{1}H-NMR spectroscopy alone can only identify the functional groups involved in the interaction without providing detailed structural information.

3.3. Computational Studies of Binding Modes between Compound 4 and Anions

The computational studies were carried for binding model of compound **4** with CN^-, F^-, $H_2PO_4^-$, and AcO^-. The interaction of the receptor compound with the CN^- anion induces changes in the molecular conformation and conformational energy of the receptor following geometry optimization. The introduction of the anion lowers the conformational energy of the interacting system relative to that of the isolated receptor, with a value of -63.17 × 10^4 kcal/mol. The interaction energy associated with the formation of the final optimized complex was calculated to be -26.956 kcal/mol.

As illustrated in Figure 8, the interaction between the receptor and the CN^- anion does not result in cleavage of the amide bond; instead, hydrogen bonding is observed during the receptor–anion interaction. The N-H bond length increases from 0.99 to 1.03 Å, while the distance between the hydrogen atom and the CN^- anion decreases from 2.50 to 1.96 Å, as summarized in Table 1. During the interaction process, the CN^- anion transiently disrupts the amide bond; however, the bond subsequently reforms, as shown in Figure 8. This phenomenon is attributed to local structural instability at that position, leading to reformation of the N–H bond.

The receptor interacting with the $H_2PO_4^-$ anion undergoes conformational changes and energy adjustments similar to those observed in its interaction with CN^- (Figure 9). Upon optimization, the addition of $H_2PO_4^-$ lowers the receptor's conformational energy to -97.64 × 10^4 kcal/mol, with a final interaction energy of -207.282 kcal/mol. As shown in Figure 9, the interaction does not

induce amide bond cleavage; instead, it leads to hydrogen-bond formation. The N–H bond distance increases from 0.99 Å to 1.04 Å, while the hydrogen atom approaches the $H_2PO_4^-$ anion from 2.50 Å to 1.70 Å (Table 2).

Across the four anions, CN^- exhibits the lowest interaction energy (-26.956 kcal/mol), indicating the most favourable binding, followed by AcO^-, F^-, and $H_2PO_4^-$. This pattern corresponds with their basicity, which follows the order $CN^- > AcO^- > F^- > H_2PO_4^-$. More basic anions have a stronger ability to accept hydrogen bonds, enhancing proton transfer and stabilizing the resulting receptor–anion complex [35].

3.4. Comparative NMR Analysis of Receptor-Anion Interactions: Experimental vs Theoretical Insights

Experimental ^{1}H-NMR analyses reveal distinct anion-dependent behavior for compound **4**. In all experiments, a water impurity signal at 1.69 ppm, originating from the $CDCl_3$ solvent, was observed. Increasing the anion concentration consistently caused a downfield shift of this water signal, indicating that water solvates the anions and reduces their effective electronegativity, thereby competing with the receptor for binding.

For the F^- and AcO^- anions, no significant chemical shift was observed for the amide proton signals, indicating that under experimental conditions, the receptor does not effectively interact with these anions. In contrast, CN^- showed partial interaction, as evidenced by a decrease in the intensity of the amide proton signal, despite negligible chemical shift, suggesting weak receptor-anion interaction in the presence of water. The $H_2PO_4^-$ anion exhibited the strongest experimental interaction with the receptor. The amine proton showed a significant downfield shift from 4.78 to 8.66 ppm ($\Delta\delta$ = 3.88 ppm), observable even at 0.5 eq. of $H_2PO_4^-$. This indicates that compound **4** is capable of effectively interacting with $H_2PO_4^-$ and can compete with water for anion binding.

Theoretical calculations predict stronger receptor -anion interactions for all four anions. For F^-, CN^-, AcO^-, and $H_2PO_4^-$, the calculated amide proton signals shift from δH = 4.72 to 15.5, 10.89, 16.54, and 12.27 ppm, respectively. These shifts indicate that, in the absence of solvation effects, the anions can approach the amide or amine groups closely, allowing for strong hydrogen-bonding interactions. The discrepancy between experimental and theoretical results is largely attributed to solvation effects in the experimental system, as water acts as a protic solvent that preferentially solvates the anions and reduces their effective binding affinity toward the receptor. In the theoretical calculations, the receptor-anion systems are modelled in the gas phase, without competing solvent interactions.

Overall, the experimental and theoretical results highlight a clear trend in receptor selectivity: $H_2PO_4^-$ interacts most strongly with compound **4**, CN^- shows moderate interaction, while F^- and AcO^- exhibit negligible interaction under experimental conditions. The consistent downfield shift of the water impurity signal across all anions further confirms the role of water in modulating receptor-anion interactions. These findings provide insight into the binding behaviour of compound **4**

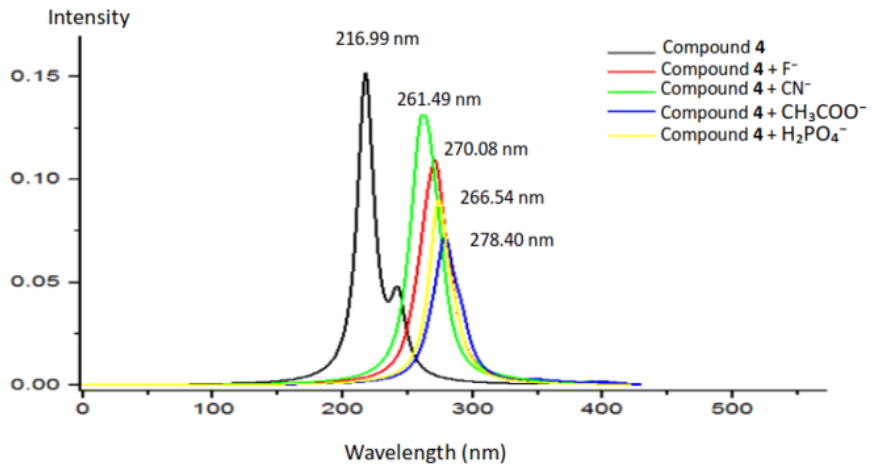

Figure 11. Theoretical UV-vis spectra of compound **4** with anions.

and its potential selectivity toward different anionic species.

The present study is limited by competitive solvent effects, particularly trace water in $CDCl_3$ and water introduced from TBA salts, which influence anion binding equilibria. Water can strongly solvate anions and compete with the receptor through hydrogen-bonding interactions, thereby reducing the experimentally observed binding response, especially for CN^- and $H_2PO_4^-$. In addition, ^{1}H-NMR provides only qualitative insight under these conditions, while gas-phase DFT calculations do not fully account for solvation and counterion effects. No crystallographic evidence is available to directly confirm the proposed binding modes. Despite these limitations, the combined experimental and computational results consistently demonstrate that compound **4** functions as a selective anion-responsive system, with the strongest response observed for CN^- and $H_2PO_4^-$ under competitive solvent conditions. The discrepancies between theory and experiment highlight the critical role of solvation and proton-transfer equilibria in governing anion recognition, providing guidance for the design of more robust and selective receptors.

3.5. Electronic Transition Shifts Revealed by UV-vis Spectroscopy: Theoretical Insights

The UV–vis results presented in this work are based entirely on TD-DFT calculations. The UV–vis titration experiments with anions were not conducted, as no visible colour change was observed upon anion addition, suggesting that the electronic transitions of compound **4** and its complexes are likely confined to the UV region. Instead, TD-DFT calculations were employed to predict the electronic transitions and possible spectral changes upon anion interaction with compound **4**. These theoretical results provide qualitative insight into changes in electronic structure upon binding or deprotonation. Accordingly, the calculated UV–vis spectra are intended to complement both the experimental and theoretical ^{1}H-NMR results by providing additional information on the electronic effects associated with anion recognition.

Hydrogen abstraction alters electronic transitions in compound **4** because the loss of a hydrogen atom localizes electron density. This effect is reflected in the UV-Vis spectra, where the absorption maximum shifts from 216.99 to 277.61 nm with a decrease in intensity (Figure 10). The electronic transitions associated with these conformational changes were calculated using TD-DFT and represented as UV-vis spectra. Hydrogen abstraction provides a reference for identifying atoms involved in receptor –anion interactions, as it highlights how conformational changes affect electronic transitions.

The UV-vis spectra of the receptor-anion complexes were calculated for optimized gas-phase conformations. Wavelength shifts were analysed to assess the impact of anion binding and to determine whether the absorption enters the visible range. None of the anions tested induced absorption in the visible region, consistent with experimental observations that no colour change occurs during receptor–anion interactions (Figure 11). The observed shifts in UV-vis spectra are associated with hydrogen-bond formation or partial deprotonation between the anion and the amide proton, which lowers the energy required for electronic transitions through electron delocalization [34]. In the compound **4**, these shifts resemble those caused by hydrogen abstraction at the amide group. The absorption maxima reveal that interactions with F^-, CN^-, AcO^-, and $H_2PO_4^-$ shift the absorption from 216.99 to 270.08, 261.49, 272.97, and 266.54 nm, respectively (Figure 11). The cleavage of covalent bonds during hydrogen abstraction and receptor-anion interaction stabilizes new conformations through electron delocalization at the amide group. This delocalization facilitates electronic transitions, resulting in wavelength shifts and a decrease in transition energy.

4. CONCLUSIONS

The combined ^{1}H-NMR and computational analyses clearly establish that *N*-(3-aminopropyl)-2-(4-allyl-2-methoxyphenoxy)acetamide (compound **4**) functions as a selective molecular receptor for CN^- and $H_2PO_4^-$ anions. The CN^- ion induces progressive deprotonation of the receptor, evidenced by complete disappearance of the amide NH signal at 8 equivalents and the NH_2 signal at 15 equivalents, confirming strong base-induced

interaction. In contrast, $H_2PO_4^-$ promotes pronounced downfield shifts (up to 3.88 ppm for NH_2), consistent with strong hydrogen-bond formation rather than full deprotonation. DFT-optimized structures corroborate these findings, showing significant shortening of N-H···anion distances and substantial downfield shifts of the amide proton, confirming strong, well-defined binding interactions specifically with CN^- and $H_2PO_4^-$. Other tested anions (F^-, AcO^-, SO_4^{2-}) do not demonstrate comparable or interpretable binding behavior under the experimental conditions. However, despite its clear molecular recognition capability, UV-vis studies reveal no bathochromic shift into the visible region, indicating that compound **4** does not function as a chromogenic sensor. Overall, compound **4** is best characterized as a selective NMR-active receptor for CN^- and $H_2PO_4^-$, with strong binding confirmed spectroscopically and computationally, but without observable colorimetric sensing ability.

AUTHOR INFORMATION

Corresponding Author

Venty Suryanti — Department of Chemistry, Universitas Sebelas Maret, Surakarta – 57126 (Indonesia); Center for Environmental Research, Universitas Sebelas Maret, Surakarta – 57126 (Indonesia);

orcid.org/0000-0003-1539-6477

Email: venty@mipa.uns.ac.id

Authors

Laras Ayu Wijayanti — Department of Chemistry, Universitas Sebelas Maret, Surakarta – 57126 (Indonesia);

orcid.org/0009-0006-3517-968X

Yoga Royandana Firdaus — Department of Chemistry, Universitas Sebelas Maret, Surakarta – 57126 (Indonesia);

orcid.org/0009-0001-1105-6910

Fajar Rakhman Wibowo — Department of Chemistry, Universitas Sebelas Maret, Surakarta – 57126 (Indonesia);

orcid.org/0000-0001-7595-7681

Ahmad Marzuki — Department of Physics, Universitas Sebelas Maret, Surakarta – 57126 (Indonesia);

orcid.org/0000-0001-8515-7522

Author Contributions

Conceptualization, Methodology, Validation, Supervision, V. S. and F. R. W.; Software, Visualization, Y. R. F; Formal Analysis, Writing - Review & Editing, V. S., F. R. W. and A. M.; Investigation, Data Curation, L. A. W. and Y. R. F.; Resources, F. R. W. and A. M.; Project Administration, L. A. W.; Funding Acquisition, Writing – Original Draft Preparation, V. S.

Conflicts of Interest

The authors declare no conflict of interest.

ACKNOWLEDGEMENT

The authors would like to thank to Universitas Sebelas Maret, Indonesia for financial support through Hibah Group Riset (Research Group Grant) with a contract number of 371/UN27.22/PT.01.03/2025.

DECLARATION OF GENERATIVE AI

Not applicable.

REFERENCES

[1] L. Chen, S. N. Berry, X. Wu, E. N. W. Howe, and P. A. Gale. (2020). "Advances in Anion Receptor Chemistry". *Chem*. **6** (1): 61–141. 10.1016/j.chempr.2019.12.002.

[2] K. Maslowska-Jarzyna, E. York, E. Feo, R. M. Maklad, G. Bao, M. Fares, and P. A. Gale. (2025). "Recent Discoveries in Anion Receptor Chemistry". *Chem*. **11** (8): 102695. 10.1016/j.chempr.2025.102695.

[3] H. Narkhede, A. Tupe, M. Kumbhare, A. Surana, and K. Khedkar. (2025). "Molecular Recognition for Anion Detection: Progress and Environmental Significance". *Intelligent Pharmacy*. **3** (6): 387–400. 10.1016/j.ipha.2025.07.001.

[4] T. S. Pandian, S. J. Cho, and J. Kang. (2013). "Dihydrogen Phosphate as a Hydrogen-Bonding Donor Element: Anion Receptors Based on Acylhydrazone". *Journal of*

Organic Chemistry. **78** (23): 12121–12127. 10.1021/jo402103d.

[5] A. Berkinbayeva, B. Kenzhaliyev, K. Smailov, A. Aimagambetov, B. Kamenov, S. Saulebekkyzy, N. Tolegenova, and P. S. R. Putri. (2025). "An Overview of Biological Cyanide Elimination from Tailing Wastewater as a Promising Tool for Sustainable Utilization". *Water Research X*. **29** : 100400. 10.1016/j.wroa.2025.100400.

[6] K. Nagaraj, A. N. Shetty, and D. R. Trivedi. (2021). "Recent Advances in the Fluorescent and Colorimetric Detection of Dihydrogen Phosphate". *Supramolecular Chemistry*. **33** (8): 408–441. 10.1080/10610278.2022.2035387.

[7] B. Barare, I. Babahan, Y. M. Hijji, E. Bonyi, S. Tadesse, and K. Aslan. (2016). "A Highly Selective Sensor for Cyanide in Organic Media and on Solid Surfaces". *Sensors*. **16** (3): 271. 10.3390/s16030271.

[8] S. Ramesh and S. Kumaresan. (2021). "A Highly Selective Coumarin-Based Chemosensor for Naked-Eye Detection of Cyanide Anions via Nucleophilic Addition in Pure Aqueous Environment". *Microchemical Journal*. **169** : 106584. 10.1016/j.microc.2021.106584.

[9] V. Suryanti, H. A. Setyono, Y. Hidayat, D. S. Black, and N. Kumar. (2025). "Synthesis, Spectroscopic Studies and Computational Modelling of Anthracene-bis-N-Acetylglyoxylic Amide Derivative for Anion Recognition". *RSC Advances*. **15** : 27772–27781. 10.1039/D5RA03382A.

[10] A. A. Veettil and S. M. Basheer. (2025). "Novel Colorimetric Anthracene-Based Thiosemicarbazone Probe for Selective Cyanide Ion Detection: From Synthesis to Real-Time Applications". *ACS Omega*. **10** (44): 52730–52744. 10.1021/acsomega.5c06461.

[11] V. Suryanti, M. Bhadbhade, H. M. Chawla, E. Howe, P. Thordarson, D. S. Black, and N. Kumar. (2014). "Novel Colorimetric Anion Sensors Based on N-Acetylglyoxylic Amides Containing Nitrophenyl Signaling Units". *Spectrochimica Acta Part A: Molecular and Biomolecular Spectroscopy*. **121** : 662–669. 10.1016/j.saa.2013.11.108.

[12] V. Suryanti, M. Bhadbhade, D. S. Black, and N. Kumar. (2017). "N-Acetylglyoxylic Amide Bearing a Nitrophenyl Group as Anion Receptors: NMR and X-Ray Investigations on Anion Binding and Selectivity". *Journal of Molecular Structure*. **1146** : 571–576. 10.1016/j.molstruc.2017.05.133.

[13] P. D. Beer and P. A. Gale. (2001). "Anion Recognition and Sensing: The State of the Art and Future Perspectives". *Angewandte Chemie International Edition*. **40** (3): 486–516. 10.1002/1521-3773(20010202)40:3.

[14] J. Gomez-Vega, A. Vasquez-Cornejo, O. Juárez-Sánchez, D. O. Corona-Martínez, A. Ochoa-Terán, K. A. López-Gastelum, R. R. Sotelo-Mundo, H. Santacruz-Ortega, J. C. Gálvez-Ruiz, R. Pérez-González, and K. O. Lara. (2024). "Thiourea-Based Receptors for Anion Recognition and Signaling". *ACS Omega*. **9** (4): 4412–4422. 10.1021/acsomega.3c06861.

[15] N. Kaur, G. Kaur, U. A. Fegade, A. Singh, S. K. Sahoo, A. S. Kuwar, and N. Singh. (2017). "Anion Sensing with Chemosensors Having Multiple NH Recognition Units". *TrAC Trends in Analytical Chemistry*. **95** : 86–109. 10.1016/j.trac.2017.08.003.

[16] F. A. Mohammed, T. Xiao, L. Wang, and R. B. P. Elmes. (2024). "Macrocyclic Receptors for Anion Recognition". *Chemical Communications*. **60** : 11812–11836. 10.1039/D4CC04521A.

[17] D. Barišić, F. Lešić, M. T. Vlašić, K. Užarević, N. Bregović, and V. Tomišić. (2022). "Anion Binding by Receptors Containing NH Donating Groups: What Do Anions Prefer?". *Tetrahedron*. **120** : 132875. 10.1016/j.tet.2022.132875.

[18] I. Ravikumar, P. S. Lakshminarayanan, and P. Ghosh. (2010). "Anion Binding Studies of Tris(2-aminoethyl)amine Based Amide Receptors with Nitro Functionalized Aryl Substitutions: A Positional Isomeric Effect". *Inorganica Chimica Acta*. **363** (12): 2886–2895. 10.1016/j.ica.2010.02.030.

[19] R. Biswas, S. Ghorai, B. Paul, S. Maji, and R. Natarajan. (2023). "Cleft Receptor for the Recognition and Extraction of Tetrahedral Oxyanions". *Crystal Growth & Design*. **23** (6): 4384–4394. 10.1021/acs.cgd.3c00167.

[20] Q. Li, Y. Yue, Y. Guo, and S. Shao. (2012). "Fluoride Anions Triggered "OFF-ON" Fluorescent Sensor for Hydrogen Sulfate Anions Based on a BODIPY Scaffold That Works As a Molecular Keypad Lock". *Sensors and Actuators B: Chemical*. **173** : 797–801. 10.1016/j.snb.2012.07.105.

[21] F. M. Pfeffer, A. M. Buschgens, N. W. Barnett, T. Gunnlaugsson, and P. E. Kruger. (2005). "4-Amino-1,8-Naphthalimide-Based Anion Receptors: Employing the Naphthalimide N-H Moiety in the Cooperative Binding of Dihydrogenphosphate". *Tetrahedron Letters*. **46** (38): 6579–6584. 10.1016/j.tetlet.2005.07.067.

[22] J. R. A. Coelho, A. R. F. Pacheco, D. C. Domingues, A. R. O. Rodrigues, A. A. Temitope, P. J. G. Coutinho, M. J. G. Fernandes, E. M. S. Castanheira, and M. S. T. Gonçalves. (2025). "New Cation Sensors Based on Eugenol-Derived Azo Dyes". *Molecules*. **30** (13): 2788. 10.3390/molecules30132788.

[23] M. Khatun, A. Sanphui, S. Malik, S. G. Chowdhury, P. Karmakar, and A. Saha. (2025). "An Eugenol-Sulfonyl Based Fluorescent Probe for Recognition of Al3+ in Real Sample Analysis and Biological Application". *Journal of Photochemistry and Photobiology A: Chemistry*. **459** : 116023. 10.1016/j.jphotochem.2024.116023.

[24] M. Khatun, J. Mandal, R. Ganguly, A. Barui, S. Banerjee, and A. Saha. (2025). "Derivative of Clove Oil Used as a Chemosensor for the Colorimetric and Fluorometric Detection of Al3+: Crystal Structure Description and Live Cell Imaging". *New Journal of Chemistry*. **49** : 3724–3735. 10.1039/D4NJ04724A.

[25] M. J. Priya, H. D. Revanasiddappa, B. Jayalakshmi, A. Swamynayaka, M. Madegowda, M. Iqbal, C. Shivamallu, K. S. Abass, R. G. Amachawadi, E. Silina, V. Stupin, and S. P. Kollur. (2025). "A Reversible Eugenol Derived Colorimetric and Fluorescence "Turn-Off" Probe for Fe2+ and Pb2+ Ions Detection". *Scientific Reports*. **15** (1): 31264. 10.1038/s41598-025-14725-2.

[26] V. Suryanti, F. R. Wibowo, and S. Handayani. (2020). "Methyl-3-(2-hydroxy-5-nitrophenyl amino)-3-phenylpropanoate Based Colorimetric Sensor for Oxyanions". *Indonesian Journal of Chemistry*. **20** (2): 257–263. 10.22146/ijc.39559.

[27] V. Suryanti, F. R. Wibowo, A. Marzuki, and M. R. K. Sari. (2020). "Cation Sensing Capabilities of a Nitrophenyl Cinnamaldehyde Derivative". *Molekul*. **15** (3): 191–198. 10.20884/1.jm.2020.15.3.654.

[28] V. Suryanti, F. R. Wibowo, T. Kusumaningsih, A. H. Wibowo, S. A. Khumaidah, and L. A. Wijayanti. (2016). "Amidation Reaction of Eugenyl Oxyacetate Ethyl Ester with 1,3 Diaminopropane". **1725** : 020085. 10.1063/1.4945539.

[29] H. Agarwalla, K. Jana, A. Maity, M. K. Kesharwani, B. Ganguly, and A. Das. (2014). "Hydrogen Bonding Interaction between Active Methylene Hydrogen Atoms and an Anion as a Binding Motif for Anion Recognition: Experimental Studies and Theoretical Rationalization". *The Journal of Physical Chemistry A*. **118** (14): 2656–2666. 10.1021/jp501769y.

[30] X. F. Sun, Z. X. Zhang, W. Li, F. Q. Bai, J. Wang, R. Jia, C. P. Kong, and H. X. Zhang. (2016). "DFT/TD-DFT Calculations on the Sensing Mechanism of a Dual Response Near -Infrared Fluorescent Chemosensor for Superoxide Anion and Hydrogen Polysulfides: Photoinduced Electron Transfer". *RSC Advances*. **6** : 104735–104741. 10.1039/C6RA23724J.

[31] G. M. Gholam, M. A. Dwicesaria, I. M. Artika, V. D. Kharisma, A. A. A. Murtadlo, S. Sahadewa, F. D. Durry, A. A. Parikesit, H. Purnobasuki, E. Volnova, Y. Lysenko, M. Rebezov, D. D. R. Turista, A. N. M. Ansori, and T. H. Sucipto. (2025). "Indonesian Herbal Compounds as Potential Inhibitors of Plasmodium falciparum CDPK2: Insights from Docking, Molecular Dynamics, and DFT Analysis". *Journal of Pharmacy and*

Pharmacognosy Research. **13** (Supplement 1): S289–S302. 10.56499/jppres25.2336_13.s1.289.

[32] M. F. Maahury, M. R. Sohilait, M. A. Martoprawiro, V. D. Kharisma, P. Listiyani, A. N. M. Ansori, S. L. Utami, A. P. Nugraha, I. Rosadi, R. S. Mandeli, M. A. Ghiffari, M. T. Albari, M. R. Ghiffari, and R. Zainul. (2023). "DFT and Molecular Docking Investigations of Curcuminoid on Tribolium castaneum Telomerase Enzyme". *Research Journal of Pharmacy and Technology*. **16** (10): 4817–4824. 10.52711/0974-360X.2023.00781.

[33] G. M. Gholam, R. A. P. Irsal, F. R. Mahendra, M. A. Dwicesaria, J. E. Siregar, A. N. M. Ansori, and R. Zainul. (2024). "In Silico Computational Prediction of Saussurea pulchella Compounds with Inhibitory Effects on Plasmepsin X in Plasmodium falciparum". *Informatics in Medicine Unlocked*. **49** : 101549. 10.1016/j.imu.2024.101549.

[34] M. A. Hossain, P. Dewan, S. M. Kawsar, A. Dangwal, K. Kalra, J. M. Kalra, P. K. Ashok, T. Parashar, V. Jakhmola, S. Saha, and A. N. M. Ansori. (2025). "Chemical Descriptors, ADMET, Molecular Docking, and Molecular Dynamics Simulation of Mannopyranoside Derivatives Against Smallpox Virus Proteins". *Advanced Journal of Chemistry, Section A*. **8** (1): 1–16. 10.48309/ajca.2025.459071.1531.

[35] S. Kundu, T. K. Egboluche, and M. A. Hossain. (2023). "Urea- and Thiourea-Based Receptors for Anion Binding". *Accounts of Chemical Research*. **56** (11): 1320–1329. 10.1021/acs.accounts.2c00701.

[36] Y. W. Liu, M. X. Kao, and A. T. Wu. (2015). "Discriminating Detection Between F− and CN− by Naked Eye from Schiff Base Sensor". *Sensors and Actuators B: Chemical*. **208** 429–435. 10.1016/j.snb.2014.11.039.

[37] M. O. Odago, D. M. Colabello, and A. J. Lees. (2010). "A Simple Thiourea-Based Colorimetric Sensor for Cyanide Anion". *Tetrahedron*. **66** (38): 7465–7471. 10.1016/j.tet.2010.07.006.

[38] S. Goswami, S. Maity, A. K. Das, A. C. Maity, T. K. Mandal, and S. Samanta. (2013). "Remarkable ESIPT-Induced NIR Emission by a Selective Colorimetric Dibenzimidazolo Diimine Sensor for Acetate". *Tetrahedron Letters*. **54** (38): 5232–5235. 10.1016/j.tetlet.2013.07.078.

[39] W. Huang, H. Su, J. Li, H. Lin, and H. Lin. (2010). "An Acetate Sensor Based on Azo in Aqueous Media". *Spectrochimica Acta Part A: Molecular and Biomolecular Spectroscopy*. **77** (1): 146–149. 10.1016/j.saa.2010.04.042.

[40] J. Shao, H. Lin, and H. K. Lin. (2008). "A Simple and Efficient Colorimetric Anion Receptor for H2PO4". *Spectrochimica Acta Part A: Molecular and Biomolecular Spectroscopy*. **70** (3): 682–685. 10.1016/j.saa.2007.08.018.

[41] N. J. Na, G. Jin-Park, H. Y. Jo, S. A. Lee, and C. Kim. (2014). "A Colorimetric Chemosensor Based on a Schiff Base for Highly Selective Sensing of Cyanide in Aqueous Solution: The Influence of Solvents". *New Journal of Chemistry*. **38** (12): 5769–5776. 10.1039/C4NJ01199F.